
Sensitivity Analysis for Inference with Partially Identifiable Covariance Matrices

Max Grazier G'Sell · Shai S. Shen-Orr ·
Robert Tibshirani

Abstract In some multivariate problems with missing data, pairs of variables exist that are never observed together. For example, some modern biological tools can produce data of this form. As a result of this structure, the covariance matrix is only partially identifiable, and point estimation requires that identifying assumptions be made. These assumptions can introduce an unknown and potentially large bias into the inference. This paper presents a method based on semidefinite programming for automatically quantifying this potential bias by computing the range of possible equal-likelihood inferred values for convex functions of the covariance matrix. We focus on the bias of missing value imputation via conditional expectation and show that our method can give an accurate assessment of the true error in cases where estimates based on sampling uncertainty alone are overly optimistic.

Keywords EM Algorithm · Semidefinite Programming · Convex Optimization · Robust Inference · cyTOF · Mass Cytometry · Flow Cytometry

1 Introduction

Methods for estimation in the presence of missing data, particularly the Expectation-Maximization (EM) Algorithm (Little and Rubin, 1987) have seen much development and use in the last several decades. One special case are data that arise from mechanisms where some pairs of variables are never observed together.

M. Grazier G'Sell
Department of Statistics, Stanford University
E-mail: maxg@stanford.edu

S. S. Shen-Orr
Department of Immunology, Rappaport Institute for Medical Research,
Bruce Rappaport Faculty of Medicine, Technion, Haifa, Israel

R. Tibshirani
Department of Health Research and Policy, Stanford University
Department of Statistics, Stanford University

This can occur in some modern biological assays, like multi-dimensional flow and mass cytometry experiments (Bendall et al, 2012), as well as in more classical setups like file matching (Rubin, 1986). Because these variables are never observed together, their partial correlation conditional on the other variables in the data set cannot be estimated. This leads to a covariance matrix that is only partially identifiable.

This issue has been addressed in several places in the literature. In the context of the EM algorithm, it is suggested that the partial correlations that are unobservable due to missingness should be assumed equal to zero (Hartley and Hocking, 1971) (Beale and Little, 1975). In practice, this may be a difficult assumption to observe. Furthermore, for modern biological applications where we believe that the unobservable partial correlations can be influential (and nonzero), it is important that we be able to assess the possible effects of these assumptions and to make robust claims in the presence of these unobservable quantities.

There has been some discussion in the literature of methods for assessing the effects of these identifying assumptions, particularly in the file matching literature. For example, Rubin (1986) and Moriarity and Scheuren (2001) both address this problem. Both of these papers assess the sensitivity of their methods to the identifying assumptions by repeating the inference with many possible proposals for the unobservable partial correlations between variables that are never observed together. As both acknowledge, it can be difficult to obtain valid and exhaustive proposals to consider. Moriarity's paper outlines one approach for obtaining them; however, it is limited to special cases that are unlikely to occur in the biological data we are considering. For large, complicated problems, the set of possible partial correlations can be quite complicated, and an automatic method for handling the ambiguity over this set would be helpful.

In the next section, we describe the details of our setup and of existing approaches, and discuss the issues and concerns that arise due to the partial identifiability of the covariance matrix. In Section 3, we propose a method for automatically conducting sensitivity analysis in this setting using semidefinite programming. In Section 4, we present simulation results and an example on biological data. Finally, in Section 5, we discuss the method, its shortcomings, and possible extensions.

2 Setup and Existing Approaches

In this section, we describe the setup and notation for our problem along with the existing estimation procedures that exist for data of this form. We discuss some of the concerns that arise in these procedures due to partial identifiability, which we address in later sections with our proposed method. Finally, we present an example and a simulation of the scenario we are discussing.

2.1 Setup and Notation

Suppose that we have latent observations $X_i^* \in \mathbb{R}^p$, $i = 1, \dots, n$, some of which may be unobserved. We will assume for this paper that

$$X_i^* \stackrel{\text{i.i.d.}}{\sim} N(\mu, \Sigma), \quad \mu \in \mathbb{R}^p, \quad \Sigma \in \mathbb{R}^{p \times p}. \quad (1)$$

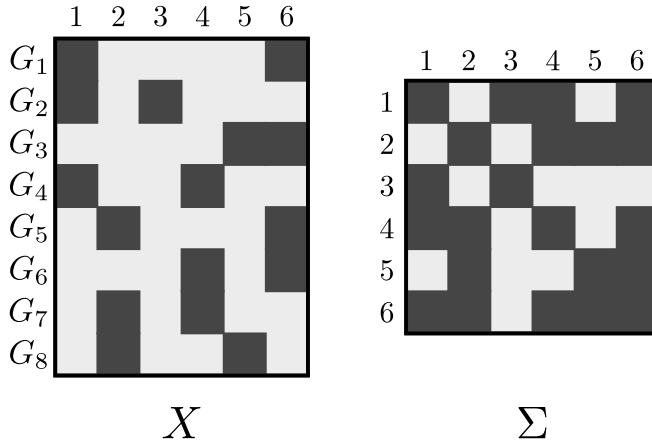


Fig. 1 A representation of the data setup. The rows of X correspond to observations, while the columns of X correspond to variables. Both indices of Σ correspond to variables. Observed entries of X are shown in black, as are the corresponding observable entries of Σ . The light gray regions of Σ cannot be determined based on the data, since those pairs never appear together in the same measurement block G_k . The indices 1 through 6 are provided to show the correspondence between the data matrix and the covariance matrix.

The observations are broken up into blocks G_1, \dots, G_K that form a partition of $\{1, \dots, n\}$. Within block G_k , only variables $J_k \subset \{1, \dots, p\}$ are actually measured. That is, our observed variable $X \in \mathbb{R}^{n \times p}$ is given by

$$X_{ij} = \begin{cases} X_{ij}^* & (i, j) \in \bigcup_k (G_k \times J_k) \\ \text{NA} & \text{otherwise} \end{cases}, \quad (2)$$

where NA refers to an observation that is censored or missing. A graphical representation of this setup is shown in Figure 1.

The case described in Equations (1) and (2) is one for which the Expectation-Maximization (EM) Algorithm is commonly used. The algorithm is detailed in Little and Rubin (1987), and described briefly in the next subsection.

We are interested in the particular case where there exist pairs of variables $j_1, j_2 \in \{1, \dots, p\}$ such that there is no J_k containing both j_1 and j_2 . This will result in inestimable partial correlations between those variables, leading the final covariance matrix to be under identified. This is discussed further in Section 2.3.

It is worth noting that another property of several of the data sources we are interested in, particularly the mass cytometry data discussed in Section 4.2, is that the number of observations in each block G_k is very large, so that the parameters corresponding to the individual blocks can be very well determined. As a result, sampling noise turns out to be less important than the partial identifiability of the covariance matrix.

Note on notation for indices. In several parts of this paper, we will be referencing sub-blocks of Σ . In those cases, indexing by sets like J_k will refer to all of the corresponding elements. For example, Σ_{J_k, J_k} refers to the sub-matrix with row and column indices in J_k , while Σ_{j, J_k} refers to the elements of row j with columns in J_k .

2.2 Estimation Approaches

The standard approach for missing data problems like these is to maximize the observed log-likelihood Little and Rubin (1987). In this case, the observed log-likelihood is given by

$$\begin{aligned} \ell_{obs}(X, \mu, \Sigma) = \text{const} &- \frac{1}{2} \sum_{k=1}^K \sum_{i \in G_k} \log |\Sigma_{J_k, J_k}| \\ &- \frac{1}{2} \sum_{k=1}^K \sum_{i \in G_k} (X_{i, J_k} - \mu_{J_k})^T \Sigma_{J_k, J_k}^{-1} (X_{i, J_k} - \mu_{J_k}) \end{aligned}$$

which is just the sum of the marginal log-likelihoods for each of the observed multivariate normal vectors.

We note here, and discuss further in Section 2.3, that this observed log-likelihood depends only on those coordinates of Σ corresponding to variables that are observed together in some block G_k . In our notation, it depends only on elements Σ_{ij} where $(i, j) \in \bigcup_k (J_k \times J_k)$.

A traditional approach to maximizing this observed log-likelihood has been the EM Algorithm, described in several places, including detailed coverage in Little and Rubin (1987). For review, we include a quick summary from their book, recast in our notation.

Let $X^{(t)}, \mu^{(t)}, \Sigma^{(t)}$ be the estimates at stage t (where $X^{(t)}$ will no longer be missing, since we will impute the values). We begin by initializing $\mu^{(1)}, \Sigma^{(1)}$. Several methods for initialization are discussed in Little and Rubin (1987). Then an iteration of the algorithm progresses as:

E-Step:

$$X_{ij}^{(t)} = \begin{cases} X_{ij} & (i, j) \in \bigcup_k (G_k \times J_k) & \text{(observed)} \\ \mathbb{E}(X_{ij} | X, \mu^{(t)}, \Sigma^{(t)}) & (i, j) \notin \bigcup_k (G_k \times J_k) & \text{(unobserved)} \end{cases}$$

M-Step:

$$\begin{aligned}\mu_j^{(t+1)} &= \frac{1}{n} \sum_{i=1}^n X_{ij}^{(t)} \\ \Sigma_{jk}^{(t+1)} &= \frac{1}{n} \sum_{i=1}^n \left((X_{ij}^{(t)} - \mu_j^{(t+1)}) (X_{ik}^{(t)} - \mu_k^{(t+1)}) + c_{jki}^{(t)} \right) \\ c_{jki}^{(t)} &= \begin{cases} 0 & X_{ij} \text{ or } X_{ik} \text{ observed} \\ \text{Cov}(X_{ij}, X_{ik} | X, \mu^{(t)}, \Sigma^{(t)}) & X_{ij} \text{ and } X_{ik} \text{ both missing} \end{cases}\end{aligned}$$

Here, conditioning on the matrix X (not $X^{(t)}$) is being used to represent conditioning on the observed, uncensored elements of the actual data X . The $c_{jki}^{(t)}$ terms in the algorithm adjust for low covariance estimates in cases where both data coordinates are missing from X . This is because using the imputed means for both coordinates would lead to inaccurately low covariance estimates.

Note that once $\mu^{(1)}$ and $\Sigma^{(1)}$ are initialized, execution of this algorithm will not be affected by the presence of partial identifiability. The previous literature addresses this problem of partially identified Σ , suggesting that the covariance matrix be initialized with the unobservable partial correlations set to zero. (Hartley and Hocking, 1971) (Beale and Little, 1975)

For certain structures of missing data, procedures for restricting these unobservable partial correlations to zero exist in the literature. This is true for factorizable designs as in Little and Rubin (1987), where the SWEEP operator is used to make the operation convenient. To the best of our knowledge, no procedure for restricting the unobservable partial correlations to zero in the EM algorithm has been set out in the literature for general designs. However, regardless of the assumptions used to make the estimation identifiable, a set of equal-likelihood estimates will exist and it is important to understand how selection among them could impact inference.

2.3 Concerns about Partial Identifiability

As noted in Section 2.1, the observed log-likelihood depends on Σ only through those elements that appear together in measurement sets J_1, \dots, J_K . Suppose that $\hat{\Sigma}$ is an estimate of the covariance matrix, in this case the result from the EM algorithm. Consider the set

$$\mathcal{S} = \left\{ \Sigma \succeq 0 : \Sigma_{ij} = \hat{\Sigma}_{ij} \text{ for } (i, j) \in \bigcup_k (J_k \times J_k) \right\}, \quad (3)$$

where $\Sigma \succeq 0$ indicates Σ in the positive semidefinite cone. Because all the matrices in this set are identical on the coordinates that appear in the observed log-likelihood, they all correspond to the same value of the observed

log-likelihood as the original estimate $\hat{\Sigma}$. Based on our data alone, there is no reason to necessarily choose one matrix in \mathcal{S} over another.

Any point estimation procedure, either implicitly or explicitly, includes an assumption on these missing elements in order to obtain a point estimate, which will be an element of \mathcal{S} by construction. The recommended practice of initializing $\Sigma^{(1)}$ in the EM algorithm to have zero for the unobservable partial correlations is one such approach. Other initializations will carry with them other implicit assumptions. These assumptions have the potential to introduce unknown biases into our estimates of Σ and into later inference that depends on these estimates.

The usual assumption for the EM algorithm is quite reasonable, as it attempts to place the estimate near the middle of the equivalence set \mathcal{S} . Nevertheless, we might wonder what effect the width of that set could have on our error. In particular, we might wonder how these unknown biases affect inference based on $\hat{\Sigma}$. The most common such inference is imputation of the missing elements of X by conditional expectation. These values are returned as part of the usual EM algorithm.

The assumptions required to identify $\hat{\Sigma}$ among the elements of \mathcal{S} could lead to an unknown bias in the imputed conditional expectations. Since this unknown bias would not be captured by sampling uncertainty, usual error estimation practices like bootstrapping could be misleadingly optimistic about the accuracy of our imputations.

2.4 Simple 3×3 Example

To illustrate the type of partial identification we are discussing, consider the following 3×3 example. This example is much simpler than the experimental settings we intend to address, but it gives a clearer understanding of the set \mathcal{S} .

Suppose that $p = 3$, and that X is made up of only two blocks of measurements. Let U, V and W be the three variables in X . We assume the structure shown in Figure 2.

In this structure, the pairs U, V and V, W have been observed together, but U and W never appear together. Thus the correlation between U and W cannot be identified, it can only be bounded by the observable correlations. The only constraint on c is that Σ is positive semidefinite. In this particularly nice example, we can work this constraint out algebraically to see that

$$c \in \left[ab - \sqrt{(1 - a^2)(1 - b^2)}, ab + \sqrt{(1 - a^2)(1 - b^2)} \right].$$

The usual recommendation that the EM algorithm estimate be constrained to zero for the unobservable correlation is equivalent in this case to constraining $c = ab$.

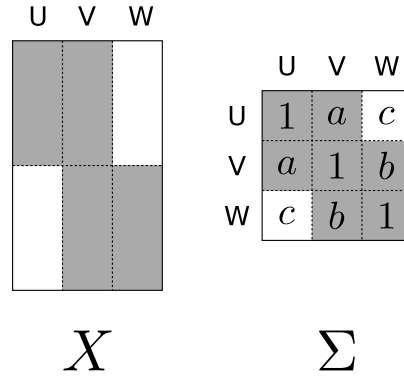


Fig. 2 Simple data structure illustrating partial identification. Variables U and W are never observed together, leading the unshaded element of Σ unidentifiable.

As a result of the lack of identifiability of c , whatever estimates \hat{a}, \hat{b} are obtained, the set

$$\mathcal{S} = \left\{ \Sigma : a = \hat{a}, b = \hat{b}, c \in \left[ab - \sqrt{(1-a^2)(1-b^2)}, ab + \sqrt{(1-a^2)(1-b^2)} \right] \right\}$$

has equal observed likelihood, so all the elements are indistinguishable based on the data alone. This is the sort of partial identifiability with which we are concerned. Any point estimate \hat{c} (for example $\hat{c} = \hat{a}\hat{b}$) corresponding to some $\hat{\Sigma} \in \mathcal{S}$ could introduce an unknown bias, both into \hat{c} and into any further inference depending on \hat{c} .

2.5 Simulation

For a more realistic example, consider the following simulation. We construct a simulated data set X drawn from a multivariate normal. For this setup, we choose $n = 5000$ samples, $p = 18$ variables, $K = 5$ groups, $|J_k| = 12$ variables measured within each group. Within each group, the 12 observed variables are chosen randomly. For our realization, this leads to nine pairs of variables that never appear together (out of 153 total pairs). Let $\mu = 0$ for convenience. To make the effect dramatic, let Σ be 1 on the diagonal, 0.3 for each of the observable entries, and 0.56 for each of the unobserved entries (chosen to keep Σ positive semidefinite). Since these unobservable entries in Σ are never measured, we expect any inference fail to take them into account. We initialize the EM algorithm with the unobserved entries set to 0.3, in agreement with all the observed entries.

We run the EM algorithm to estimate $\hat{\Sigma}$. The plot in Figure 3 shows the resulting estimates for the unobservable elements of Σ , along with the true value. We see that the estimates miss the true value, as we would expect.

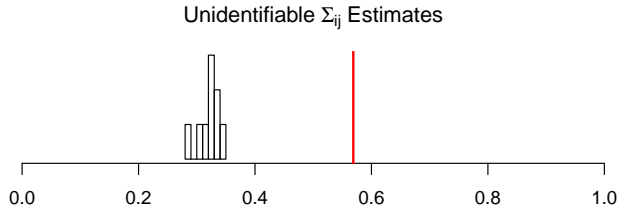


Fig. 3 The histogram shows the estimates for the unidentified elements of Σ , while the vertical red line shows the true value in our simulation.

As a demonstration, we consider ten realizations of the previous simulation. For each, we look at the imputed and actual values for the missing coordinates in the first row of X . These are shown in Figure 4. We see that the sampling uncertainty does not capture the actual error from the true value, which is quite large in some cases. This suggests that, in this setting, the unknown error due to the ambiguity in \mathcal{S} is important to understand.

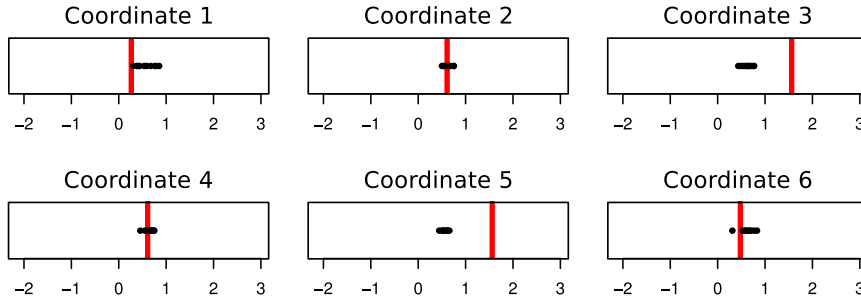


Fig. 4 Each subplot shows the ten imputed values for a missing element of X , based on ten different realizations of the simulation. The vertical red lines show the true values for those coordinates. We see that the sampling uncertainty in the imputations is very small, but that it does not capture the missing bias due to the estimation assumptions.

In the next section, we propose an approach to determining the sensitivity to the set \mathcal{S} of inference based on Σ , so that this error can be understood and bounded.

3 Sensitivity Analysis by Semidefinite Programming

From the previous section, we recognize that because some pairs of variables are never observed together, any estimate $\hat{\Sigma}$ has a set of equivalently likely

estimates

$$\mathcal{S} = \{\Sigma \succeq 0 : \Sigma_{ij} = \hat{\Sigma}_{ij} \text{ for } (i, j) \in \bigcup_k (J_k \times J_k)\}$$

which are indistinguishable based on the data. Any point estimate of Σ must choose a particular element of \mathcal{S} , which in turn can lead to an unknown bias in inference based on Σ .

Accepting the ambiguity of \mathcal{S} as an inherent shortcoming of the lack of coverage of our measurements, we would still like to be able to capture the range of possible values in our inference. We saw in Figure 4 that the usual methods for estimating sampling error, like the bootstrap, will not address this bias. In this section we propose and describe a method for sensitivity analysis in this setting, giving bounds on the range of imputed values with respect to all of \mathcal{S} .

3.1 General Approach

Our goal here is to bound the values obtained by inference on Σ over the entire set \mathcal{S} . It is convenient to notice that \mathcal{S} is the intersection of the convex semidefinite cone $\{\Sigma \in \mathbb{R}^{p \times p} : \Sigma \succeq 0\}$ with the affine set $\{\Sigma \in \mathbb{R}^{p \times p} : \Sigma_{ij} = \hat{\Sigma}_{ij} \text{ for } (i, j) \in \bigcup_k (J_k \times J_k)\}$. As a result, \mathcal{S} itself is a convex set.

We are interested in understanding the effect of the under-identified nature of Σ on inferred quantities based on Σ . The example given above, and which we will continue to use, is that of imputation by conditional expectation. For a general inferred quantity $f(\Sigma)$ (potentially also a function of X and μ), we can look at extrema of the function f over \mathcal{S} . For the case of convex or affine f , this can be tractable because of the convexity of \mathcal{S} , and we will be able to bring to bear machinery from the study of convex optimization and particularly semidefinite programming. Finding such extrema will give bounds on the range of possible values of f over the entire set \mathcal{S} of likelihood maximizing matrices.

In the next subsection, we expand on this idea for the case where f is the conditional expectation. We will return to general applications briefly in the discussion in Section 5.

3.2 Algorithm: Conditional Expectation

In this section, we are interested in applying the idea from Section 3.1 to conditional expectation, particularly the imputations of the missing values in X . For this section, we fix i and j so X_{ij} is the missing element we would like to impute, and we fix k so that $i \in J_k$ and $j \notin J_k$. The quantities of interest then take the form

$$f(\Sigma) = \mathbb{E}(X_{ij} | X_{iJ_k}) = \mu_j + \Sigma_{jJ_k} \Sigma_{J_k J_k}^{-1} (X_{iJ_k} - \mu_{J_k}), \quad (4)$$

corresponding to the conditional expectation of the i^{th} row and j^{th} column of X . This section focuses on understanding the range of possible values for (4) for $\Sigma \in \mathcal{S}$.

The quantity in (4) appears to be non-convex in Σ . However, we are interested in optimizing it only over $\Sigma \in \mathcal{S}$. Within \mathcal{S} , the block Σ_{J_k, J_k} is held constant, since it corresponds to coordinates that are observed together in block G_k . This means that as long as $\Sigma \in \mathcal{S}$, Σ_{J_k, J_k} is fixed and can be set to $\hat{\Sigma}_{J_k, J_k}$, the corresponding block of our initial estimate (e.g., from the EM algorithm). This results in the simplified version of the objective from Equation (4),

$$f(\Sigma) = \mathbb{E}(X_{ij}|X_{iJ_k}) = \mu_j + \Sigma_{jJ_k} \hat{\Sigma}_{J_k, J_k}^{-1} (X_{iJ_k} - \mu_{J_k}). \quad (5)$$

This is not only convex in Σ over \mathcal{S} , but is affine. As a result, (5) has both unique maxima and unique minima over \mathcal{S} .

Finding the range of possible imputed values is then equivalent to solving the semidefinite program (SDP)

$$\begin{aligned} & [\min/\max]_{\Sigma} \text{imize } \Sigma_{j, J_k} \hat{\Sigma}_{J_k, J_k}^{-1} (X_{J_k} - \hat{\mu}_{J_k}) \\ & \text{subject to } \Sigma \succeq 0 \\ & \Sigma_{ab} = \hat{\Sigma}_{ab} \text{ for } (a, b) \in \bigcup_{\ell} (J_{\ell} \times J_{\ell}) \end{aligned}$$

Here we have dropped the μ_j term for conciseness, since it is just a constant and can be reintroduced later.

The algorithm for finding the minimum and the maximum of this affine function will be the same, so we will just focus on the minimum here. To solve the SDP, we will replace the semidefinite cone constraint ($\Sigma \succeq 0$) with a log-barrier (Boyd and Vandenberghe, 2004). As t grows large, the following minimization problem is equivalent to the original one.

$$\begin{aligned} & \underset{\Sigma}{\text{minimize}} \quad -\frac{1}{t} \log |\Sigma| + \Sigma_{j, J_k} \hat{\Sigma}_{J_k, J_k}^{-1} (x_{J_k} - \hat{\mu}_{J_k}) \\ & \text{subject to } \Sigma_{ab} = \hat{\Sigma}_{ab} \text{ for } (a, b) \in \bigcup_{\ell} (J_{\ell} \times J_{\ell}). \end{aligned}$$

To solve the original SDP, we solve this minimization problem over a sequence of increasing t with warm starts (see Appendix A for details). The preceding optimization problem becomes the inner loop of the algorithm. Each minimization is computed by generalized gradient descent. Furthermore, we apply recent approaches for accelerating gradient descent, for example in Banerjee et al (2006) and Beck and Teboulle (2010), to speed up convergence. The timings below show that this acceleration provided much faster convergence times. The details of the algorithm can be found in the appendix to this paper.

Timings. Timings on a variety of problem sizes are shown in Figure 5. A comparison is made between generalized gradient descent with and without acceleration. These simulations are all run on a 3.3Ghz Intel Xeon X5680 processor.

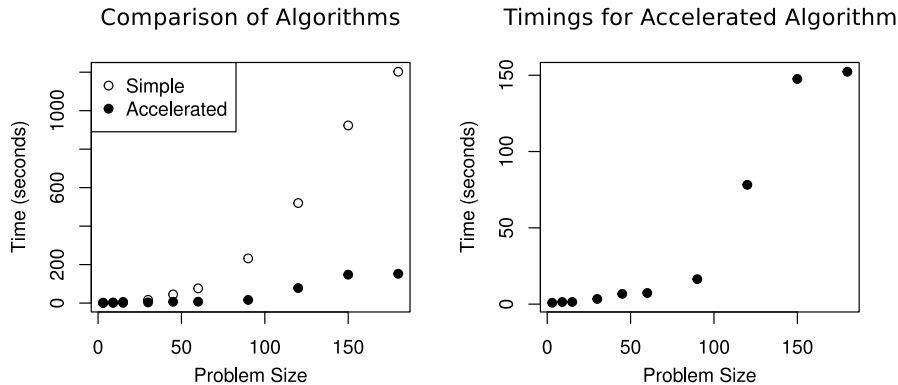


Fig. 5 Time in seconds to compute upper and lower bounds for one imputed entry. This involves executing the SDP algorithm twice. Each entry is an average over ten repetitions.

The limiting computation at each step of the algorithm is a singular value decomposition to compute the inverse and check the step size conditions, at a cost of $O(p^3)$. We see that the computation is possible through p in the low hundreds. The accelerated form of the algorithm is an order of magnitude faster on large problems, since it requires fewer iterations to converge to the solution and thus fewer costly matrix decompositions.

It is worth noting that computing these bounds for all the missing coordinates of X could become quite expensive. Conveniently, the algorithm is quite parallelizable, since the entries of each row of X can be bounded with no information sharing from other rows. This makes the algorithm well-suited to being distributed over large computing clusters. The authors are interested in pursuing this possibility to make even large problems accessible for this method.

4 Results

In this section, we give results from the proposed algorithm for sensitivity analysis of the imputed conditional expectations. The first example is the same simulation setup as outlined in Section 2.3 and shown in Figures 3 and 4. The second is mass cytometry data, which was the setting that inspired our interest in this problem.

4.1 Simulation

The simulation setting is the same as outlined in Section 2.3. We run the same simulation as in Figure 4, looking at the true and imputed conditional means. As in the first simulation, we do this for 10 realizations of the data, looking at the six imputed values in the first row of X .

This time, we use the SDP algorithm above to obtain a range of possible imputed values over all of \mathcal{S} . This gives bounds on the bias due to assumptions on the missing partial correlations.

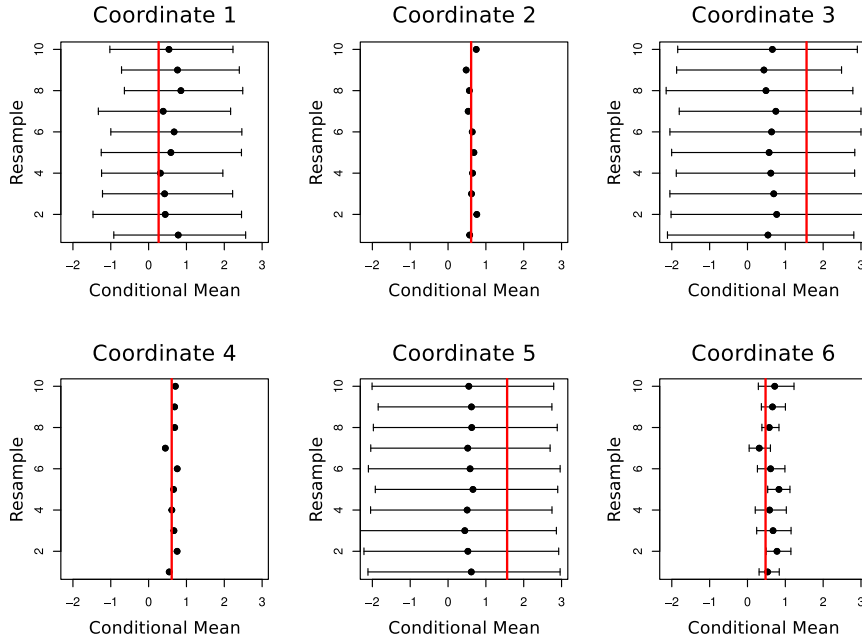


Fig. 6 Imputed values over 10 realizations are shown as black dots. The computed range of possible imputed values due missing partial correlations is shown by black intervals. The vertical red lines are the true conditional means.

We see in Figure 6 that the intervals cover the true values, capturing the unobservable bias. The method gives an indication of the reliability of particular imputations, taking into account how well the relevant correlations are constrained by the observable ones. Coordinates 2 and 4 depend only on observable correlations, so their intervals have zero length since \mathcal{S} is degenerate. Coordinates 3 and 5 have very wide intervals and are quite conservative, but this is merely a realistic assessment of the data structure's inability to constrain the correlations of interest. These are examples of the wide intervals our method can produce. While it would be desirable to have shorter intervals, it is

not possible. The wide intervals produced by our approach correspond to estimates that are all indistinguishable based on the data; there is no information in the data to distinguish between points in the intervals.

In cases like coordinate 1 and particularly coordinate 6, the method gives quite narrow ranges, indicating that the relevant correlations have been well-constrained by the estimable correlations, giving reliable imputations. This is valuable information to have, especially in settings where we expect strong correlations to occur, like biology. Our next section gives an example using mass cytometry data, where data with this missing structure arise inherently.

4.2 Real Mass Cytometry Data

Our interest in this area was originally inspired by mass cytometry data from Time-of-Flight (cyTOF) experiments. The structure of the data in those experiments lends itself to the designs we have described in Section 2.1. The technology is described in detail in Bendall et al (2012). We will give a brief overview below. We note that though we discuss the ideas presented here in the context of newer mass cytometry technology, they would in principle be applicable to the more established fluorescence based flow cytometry technology.

Mass cytometry experiments run on a cyTOF machine measure protein expression of many proteins on a single cell basis. This is done by attaching tagged antibodies to the cells, which bind to specific proteins. Each protein specific antibody is tagged with heavy metal atoms of a specified type. The cells are then atomized one at a time and sent through a mass spectrometer. The mass spectrometer measures all of the heavy metal tags present, each reflecting the abundance of expression of a specific protein in each cell.

The data structure that we have been discussing arises because, while there are several hundreds of proteins of interest, there are only a limited number of different heavy metals that can be bound to these antibodies. As of this article, the state of the art is 45 unique metal tags (Bendall et al, 2012) and 17 unique fluorescent tags in flow cytometry (Chattopadhyay et al, 2006).

To study more proteins, one could construct several different sets of antibody tags, each using the same metals to code for different proteins. The cell population can then be divided into batches, and each can be run against a different set of probes.

This setup is illustrated in Figure 7. It yields a structure of missingness in the data just as we have described above. Each batch of cells corresponds to a group of observations G_1, \dots, G_K , while each set of probes and resulting measurements corresponds to a set of observable variables J_1, \dots, J_K .

As experiments of this form are only beginning to be run, we use existing data sets to simulate data of this form. Evan Newell provided us with the data used in Newell et al (2012). We focus on a particular data set of mass cytometry measurements on proteins from a blood sample of one patient. Lab procedures were used to obtain a reasonably homogeneous sample of cells.

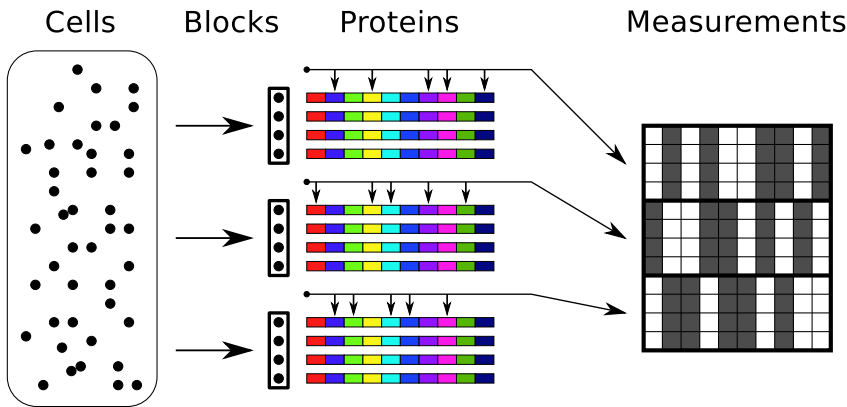


Fig. 7 Representation of the mass cytometry data acquisition. The incoming cells are grouped into blocks. Each block is measured with a unique set of probes, which measure a subset of the available proteins. The protein colors represent protein identity; although some amount of each protein may be present in each cell, the probes can only measure a subset of the protein types. This measurement scheme leads to the data matrix X , shown on the right, with observed data shaded grey.

The data set then consisted of measurements of 34 proteins on 43,700 cells. We divide this data set randomly into five smaller data sets to give some sense of the variation in the methods we will apply. To create missingness patterns of the desired type, we break each subset into 10 groups, and within each group we artificially censor 10 of the proteins, leaving measurements of only 24 of the 34 proteins. Because of the skewness of the measurement distributions, we work with the logarithm of the mass cytometry measurements.

To illustrate the problems that can occur with missing pairs, we select the top 5% of correlations from the full dataset, and ensure that the corresponding pairs of variables never appear together in the same group of variables. This means that the corresponding partial correlations will be under-determined.

To give the EM algorithm a favorable starting point, we begin with the true covariance matrix for the full data set. We hold fixed those elements corresponding to variables which have been observed together, and change the other elements to place the matrix near the center of the cone (similar to making the corresponding partial correlations zero). We do this by minimizing $\log |\Sigma|$ while holding the identifiable elements fixed.

For each of these synthetic data sets, we execute both the EM algorithm and our SDP algorithm. Figure 8 shows the resulting estimates for the missing proteins in the first row of X . For comparison, we show the true conditional means for the missing entries, computed using the full covariance matrix with no missing data.

In plot (a), we see that the sampling uncertainty does not capture the error from the true conditional mean. However, the interval estimates reveal

Imputation Results for Real Mass Cytometry Data

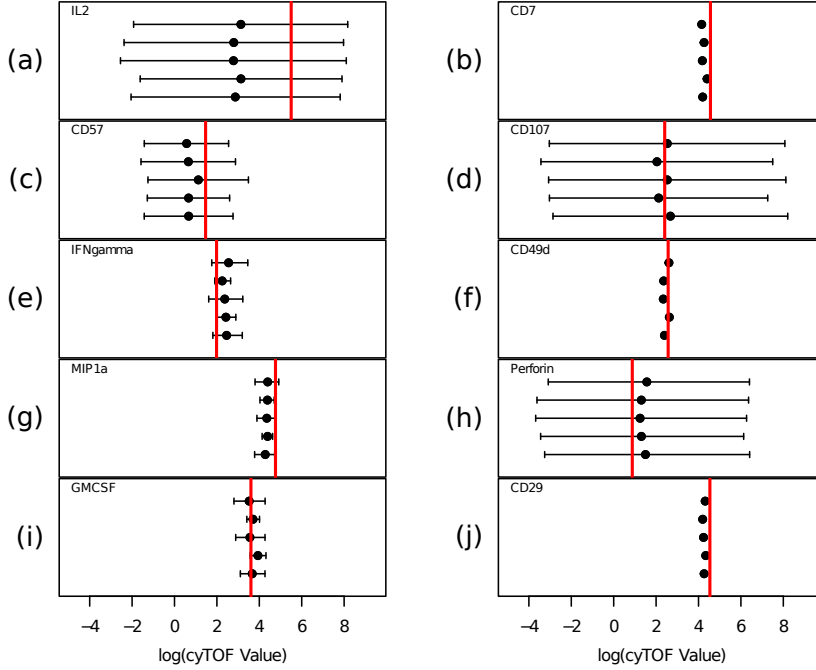


Fig. 8 Results for 10 inferred proteins across 5 identically distributed synthetic data sets. Each plot shows the 5 identically distributed realizations. The imputed EM estimates are shown by black dots. The SDP computed range of possible imputed values due to missing partial correlations is shown by the black intervals. The red vertical line shows the true conditional mean, given the full population covariance matrix from the 43,700 completely observed cells.

the potential bias in the estimator. The error to the true mean falls within this range of potential bias.

In other cases, like (b), (f) and (j), the intervals have zero width, because the equivalence set \mathcal{S} is degenerate. This indicates that sampling uncertainty should be an accurate measure of the error, which it turns out to be. Similarly, in (e), (g), (i) and to a lesser extent in (c), we obtain non-degenerate intervals that have small widths, indicating a small potential bias.

In cases (d) and (h), our algorithm indicates the potential for very large biases to be present in the estimator. Knowing the true mean, we see that this did not occur. We expect this conservative behavior in some cases. Our algorithm considers the set of possible imputed values over all likelihood-equivalent matrices. There is no reason to believe that the true unobserved covariance will correspond to imputed values that are near the edge of all of these intervals.

In this data, we see that it is possible for the lack of identifiability due to the data structure to lead to errors in imputation that are not captured

by the sampling uncertainty. In cases where the sampling uncertainty does not capture the error from the true conditional mean, our interval estimates reveal the potential for bias in the estimator. Where our interval estimates are small, we see that the EM estimates are within sampling uncertainty of the true value. This provides evidence that the intervals computed using our algorithm, though conservative, do capture these errors in imputation due to lack of identifiability in the data structure.

5 Discussion

This article addresses the issue of missing data imputation by the EM algorithm in the case where some partial correlations are unobservable, resulting in an under-identified covariance matrix. We propose an automatic method for sensitivity analysis of the resulting imputations to the assumptions being made on those unobservable correlations. We present a semidefinite program that computes the range of possible imputations over the convex set of equal likelihood covariance estimates. We see from simulation and real biological data that this gives an accurate sense of the possible errors due to identifying assumptions.

Sensitivity analysis for problems of this nature has been previously discussed in the literature, including Rubin (1986) and Moriarity and Scheuren (2001). The method in this paper differs in that it automatically handles the problem of exploring the set of consistent correlation structures, and finds the actual extrema over that set. To the best of our knowledge, previous approaches have not automatically explored this space.

The method outlined here could be combined well with methods like bootstrapping for estimating the uncertainty due to sampling, which would give intervals that were robust to both sampling uncertainty and identifying assumptions. It is also worth noting that our method computes the extrema separately for each conditional mean to be imputed. This is bound to be conservative, as the $\Sigma \in \mathcal{S}$ that maximizes or minimizes the conditional expectation for one coordinate in X is not likely to correspond to the extrema of another coordinate.

We saw in the results in Section 4 that the intervals have the potential to be very wide, if the data were collected in a way that poorly constrains the important correlations. This suggests that care should be taken, when possible, to design the data missingness to constrain important quantities of interest. We believe that the method in this paper could be used to give a better idea of the possible imputation error and to guide the design of the experiments. Mass cytometry experiments, discussed in Section 4.2, are very amenable to this type of design. The authors are presently working on experimental design for mass cytometry data to control the identifiability issues discussed in this paper.

Finally, much of this paper focuses on bounding the potential error due to partial identifiability of Σ in the case of imputation by conditional expectation.

It could be interesting to consider other quantities that could be bounded over the set \mathcal{S} in a similar fashion. The quantities that can be easily handled are constrained by the need that they be convex over \mathcal{S} .

This can include functions like Mahalanobis distance and variance components $u^T \Sigma u$ (for fixed u). This leads to applications that rely on those measures. For example, in Principle Component Analysis (PCA), for a given component u , one could bound the range of possible variances in that direction over the set \mathcal{S} by optimizing the affine function $u^T \Sigma u$. Similarly, in single-linkage clustering using Mahalanobis distance, minimizations of $u^T \Sigma^{-1} u$ could be used to give a lower bound on the separation of the resulting clusters.

Acknowledgements The authors would like to thank Noah Simon for discussion of optimization methods and Jacob Bien for other helpful discussions. We would also like to thank Sean Bendall and Erin Simons for first posing the problem to us, and Evan Newell for providing us with the mass cytometry data.

MGG is supported by a National Science Foundation GRFP Fellowship. SSSO is a Taub fellow and is supported by US National Institutes of Health (NIH) (U19 AI057229). RT was supported by NSF grant DMS-9971405 and NIH grant N01-HV-28183.

References

- Banerjee O, El Ghaoui L, d'Aspremont A, Natsoulis G (2006) Convex optimization techniques for fitting sparse gaussian graphical models. In: ACM International Conference Proceeding Series, Citeseer, vol 148, pp 89–96
- Beale E, Little R (1975) Missing values in multivariate analysis. *Journal of the Royal Statistical Society Series B* 37(1):129–145
- Beck A, Teboulle M (2010) Gradient-based algorithms with applications to signal recovery problems. *Convex Optimization in Signal Processing and Communications*, ed DP Palomar and YC Eldar pp 42–88
- Bendall SC, Nolan GP, Roederer M, Chattopadhyay PK (2012) A deep profiler's guide to cytometry. *Trends in immunology* 33(7):323–332
- Boyd S, Vandenberghe L (2004) *Convex optimization*. Cambridge University Press, New York
- Chattopadhyay P, Price D, Harper T, Betts M, Yu J, Gostick E, Perfetto S, Goepfert P, Koup R, De Rosa S, et al (2006) Quantum dot semiconductor nanocrystals for immunophenotyping by polychromatic flow cytometry. *Nature medicine* 12(8):972–977
- Hartley H, Hocking R (1971) The analysis of incomplete data. *Biometrics* 27(4):783–823
- Little R, Rubin D (1987) *Statistical analysis with missing data*. Wiley, Hoboken
- Moriarity C, Scheuren F (2001) Statistical matching: a paradigm for assessing the uncertainty in the procedure. *Journal of Official Statistics-Stockholm* 17(3):407–422
- Newell EW, Sigal N, Bendall SC, Nolan GP, Davis MM (2012) Cytometry by time-of-flight shows combinatorial cytokine expression and virus-specific cell

niches within a continuum of cd8+ t cell phenotypes. *Immunity* 36(1):142 – 152, DOI 10.1016/j.immuni.2012.01.002

Rubin DB (1986) Statistical matching using file concatenation with adjusted weights and multiple imputations. *Journal of Business & Economic Statistics* 4(1):pp. 87–94

A Algorithmic Details

From Section 3.2, the inner optimization problem we wish to solve is

$$\begin{aligned} & \underset{\Sigma}{\text{minimize}} && -\frac{1}{t} \log |\Sigma| + \sum_{j, J_k} \hat{\Sigma}_{J_k, J_k}^{-1} (x_{J_k} - \hat{\mu}_{J_k}) \\ & \text{subject to} && \Sigma_{ab} = \hat{\Sigma}_{ab} \text{ for } (a, b) \in \bigcup_{\ell} (J_{\ell} \times J_{\ell}). \end{aligned}$$

This optimization problem, with fixed t , can be solved by generalized gradient descent. The gradient of the objective is

$$\begin{aligned} \nabla(\text{objective}) &= -\frac{1}{t} \Sigma^{-1} + C \\ C_{ab} &= \begin{cases} \left(\hat{\Sigma}_{J_k, J_k}^{-1} (x_{J_k} - \hat{\mu}_{J_k}) \right) [b] & a = j \text{ and } b \in J_k \\ \left(\hat{\Sigma}_{J_k, J_k}^{-1} (x_{J_k} - \hat{\mu}_{J_k}) \right) [a] & a \in J_k \text{ and } b = j \\ 0 & \text{otherwise} \end{cases} \end{aligned}$$

If we initialize the first time with $\Sigma = \hat{\Sigma} \in \mathcal{S}$, we want to remain within \mathcal{S} with each step. Therefore, we project the gradient into the linear space $\{\Sigma : \Sigma_{ij} = \hat{\Sigma}_{ij} \forall (i, j) \in \bigcup_k (J_k \times J_k)\}$. This is equivalent to holding the coordinates $(i, j) \in \bigcup_k (J_k \times J_k)$ fixed, and only taking gradient steps in the other directions.

With a step size of δ , the update becomes

$$\begin{aligned} \Sigma_{ab}^{(t+1)} &= \Sigma_{ab}^{(t)} + \delta \left(\frac{1}{t} (\Sigma^{(t)})_{ab}^{-1} - C_{ab}^{(t)} \right) && (a, b) \notin \bigcup_{\ell} (J_{\ell} \times J_{\ell}) \\ \Sigma_{ab}^{(t+1)} &= \Sigma_{ab}^{(t)} && (a, b) \in \bigcup_{\ell} (J_{\ell} \times J_{\ell}) \end{aligned}$$

Using warm starts, we repeatedly solve this problem with increasing t to obtain the final solution. This barrier method is discussed in Boyd and Vandenberghe (2004), which recommends using a sequence of t that increase by a factor of μ (around 10-20) at each outer loop iteration. More details of the method can be found in Section 11.3.1 of that book.

We also include acceleration, as in Banerjee et al (2006) and Beck and Teboulle (2010), among others. This is shown in Figure 5 to give practically significant improvements in algorithm timings. The final algorithm is shown in Algorithm 1.

```

Input: The estimated covariance matrix  $\hat{\Sigma}$ 
Initialize  $\Sigma$  and  $\Theta$  to  $\hat{\Sigma}$ 
Initialize  $\ell = 1$ 
Define  $C$  as in Section 3.2
for  $t = t_0$  to  $t_f$  do
  repeat
     $G_{ab} = \frac{1}{t} (\Sigma)_{ab}^{-1} - C_{ab}$  for  $(a, b) \notin \bigcup_{\ell} (J_{\ell} \times J_{\ell})$ 
     $\Sigma_{old} = \Sigma$ 
    Compute appropriate  $\delta$ 
     $\Sigma = \Theta + \frac{\ell}{\ell+3} (\Sigma - \delta G - \Theta)$ 
     $\Theta = \Sigma_{old} - \delta G$ 
     $\ell = \ell + 1$ 
    if  $\ell > \ell_{max}$  then
      |  $\ell = 1$ 
    end
  until  $\max_{a,b} |\Sigma_{ab} - (\Sigma_{old})_{ab}| < \varepsilon$ 
end

```

Algorithm 1: Accelerated algorithm for solving the SDP in Section 3.2. The variable Θ is introduced to carry information about the previous steps for the momentum term. We include restarts in the momentum weight every ℓ_{max} steps, which empirically improves performance. The procedure for computing an appropriate δ is shown in Algorithm 2.

Some care needs to be taken in selecting the step size δ . We choose it by backtracking to result in a decrease in the objective, to remain inside the positive semidefinite cone, and to satisfy the majorization requirements of generalized gradient descent (Beck and Teboulle, 2010). This sub-algorithm is shown as Algorithm 2.

```

Input :  $\Sigma, G$ 
Initialize  $\delta = 1/0.8$ 
repeat
   $\delta = 0.8\delta$ 
   $\Sigma_{test} = \Sigma - \delta G$ 
   $\lambda_{min} = \min\{\text{eigenvalues}(\Sigma_{test})\}$ 
   $f_{obj} = -\frac{1}{t} \log |\Sigma_{test}| + (\Sigma_{test})_{j, J_k} \Sigma_{J_k, J_k}^{-1} (x_{J_k} - \hat{\mu}_{J_k})$ 
   $f_{maj} = -\frac{1}{t} \log |\Sigma| + \Sigma_{j, J_k} \Sigma_{J_k, J_k}^{-1} (x_{J_k} - \hat{\mu}_{J_k}) + G \circ (\Sigma_{test} - \Sigma)$ 
   $\quad + \frac{1}{2\delta} (\Sigma_{test} - \Sigma) \circ (\Sigma_{test} - \Sigma)$ 
until  $\lambda_{min} \geq 0$  and  $f_{obj} \leq f_{maj}$ 
Output:  $\delta$ 

```

Algorithm 2: Sub-algorithm to compute appropriate step size δ . We use $A \circ B$ to denote the Frobenius inner product, $\sum_a \sum_b A_{ab} B_{ab}$.